Preprints of the 19th World Congress
The International Federation of Automatic Control
Cape Town, South Africa. August 24-29, 2014

Modelling and Decentralized Adaptive Model Predictive Control for Alumina Trihydrate Precipitation Process

LIU Zheng*. PENG Xiao-qi. SONG Yan-po*****

**School of Information Science and Engineering, Central South University, Changsha, CO 410083 China (Tel:86-0731-88836713; e-mail: liuzhenglady@163.com).*
***Hunan First Normal University, Changsha, CO 410205 China (e-mail: pengxq126@126.com)*
**** School of Energy Science and Engineering, Central South University, Changsha, China, (e-mail: songyanpo@csu.edu.cn)}*

Abstract: This paper presents a decentralized adaptive model predictive control scheme for alumina trihydrate precipitation process that is a large-scale nonlinear complex system with strong disturbances and a large time constant. The overall precipitation system is decomposed into several small-scale systems expressed as several Hammerstein structures with an adaptive disturbance model. The local controller takes the upstream state into account as a measured disturbance. The proposed method preserves the small computation and communication properties of decentralized MPC while ensuring a good performance. A simulation based on real data shows the model is true and the control method is effect.

Keywords: Control for large-scale systems, Decentralized model predictive control, Process modeling.

1. INTRODUCTION

The alumina trihydrate precipitation step determines the alumina productivity and quality in the commercial Bayer process. The main function of the precipitation step is to gain alumina trihydrate crystals from the agitated and supersaturated sodium aluminate solution in the presence of large quantity of gibbsite seed at the proper temperature. Many studies show that the precipitation crystal yield and size distribution are affected by the precipitation temperature to a great extent (Yamada; Satapathy; Yanly). Though precipitation temperature is a key plant process condition, the temperature is not controlled automatically but manually in the industrial production at present, and the performance of manual temperature control is bad. Because the precipitation process is a large-scale nonlinear complex system with strong disturbances and a large time constant, the traditional control technology can not apply to this process successfully. Implementation of an accurate automatic control has become an urgent problem in production.

In recent years, model predictive control (MPC) was widely and successfully applied in controlling complex industrial processes, showing its great potential in handling complex constrained optimization control problems (Qin; XI). However, large-scale systems are often hard to be controlled in a centralized way due to the excessive computational burden and the difficulty in constructing and maintaining a full dynamical model for control design. Hence, decentralized or distributed MPC (DMPC) for large scale systems is a new trend. Christofides et al. (Christofides; Scattolini) review a number of decentralized, distributed and hierarchical MPC architectures for large scale systems and provide many algorithmic details. Some DMPC algorithms were proposed base on a set of assumption like no model errors, no disturbances or constraints and so on (Wang; Magni). Though these algorithms provide a good theoretical performance, the good performance may not be achieved in the real precipitation process with strong nonlinearity and unmeasured disturbances. Some DMPC methods were designed for power system (Mohamed; Moradzadeh). These controlled systems are quite different from the precipitation process, so that the DMPC methods for them do not suit to control the precipitation process. Liu and Heidarinejad used a Lyapunov-based MPC controller as the local controller to preserve the stability properties while satisfying input constraints, and on this basis they developed different kinds of DMPC scheme and the theoretical results are demonstrated through a nonlinear chemical process example (Liu,2010; Heidarinejad,2011a,b). However they did not discuss the situation in which the strong unmeasured disturbances exist. Mercangoz proposed a DMPC framework based on a stable Nash equilibrium. The framework is demonstrated on an experimental four-tank system (Mercangoz). The results show the method performs significantly better than a completely decentralized set of controllers. However the DMPC application introduces a communication overhead. Furthermore, the main performance improvement depends on the repetition of the optimization problems which introduces additional computational load. Zheng proposed a DMPC framework based on neighbour-hood optimization, and applied it to an accelerated cooling process in a test rig (Zheng, 2009, 2011). The local controller only communicates with its neighbour controllers and adapts a linear model as local predictive model, which reduce the computational and communicational burden. However the iteration of the

optimization problem is obligate. A comparative analysis shows that the distributed scheme is not necessarily better than a decentralized scheme because it depends on the formulation of the controller and its design (Alvarado). If steady-state errors were not taken into account, the decentralized scheme shows the shortest settling time and the best transient performance.

In this paper we proposed a decentralized adaptive MPC scheme for the precipitation process. The local predictive model has a Hammerstein structure with adaptive disturbances model, and the local controller takes the upstream state into account as a measured disturbance, which preserves the advantage of the decentralized scheme while improving the steady-state performance. This decoupling scheme makes the performance of each subsystem control loop independent of other subsystem control loops and simplifies the MPC controller design. The introduction of upstream state and the adaptive disturbances model ensures the steady-state performance and a stronger rejection of disturbances.

The contents are organized as follows. Section 2 describes the alumina trihydrate precipitation process. Section 3 establishes the first principles process model. Section 4 presents the proposed decentralized adaptive MPC scheme. A real production data based simulation is presented in Section 5. Finally, a brief conclusion is drawn to summarize the study.

2. ALUMINA PRECIPITATION PROCESS DESCRIPTION

Fig.1 illustrates the precipitation process. The supersaturated sodium aluminate solution and gibbsite crystal seeds are fed into the first precipitator, and mixed by continuous stirring. The feed slurry flows through a series of precipitators by its own weight, the exothermic crystallization reaction occurring under atmospheric pressure. The precipitator is made of steel, so it is easy to exchange heat with the environment. A thermometer is located at the outlet of each precipitator to measure the temperature of the slurry. Some wide-runner plate heat exchangers are mounted on the top of precipitators to cool the slurry. The slurry is pumped from the precipitator to the heat exchanger, and exchange heat with the cooling water, then return to the precipitator. The inlet temperatures, outlet temperatures and flow rates of both fluids flowing through the heat exchanger can be measured. The cooling water flow can be controlled by the electrically operated valve.

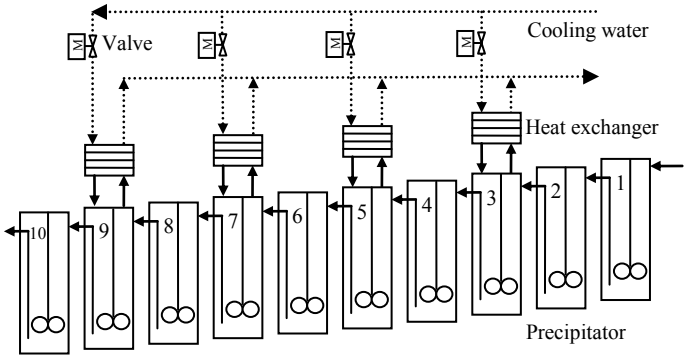

Fig.1 Alumina precipitation process

3. MODEL

3.1 Dynamic Model of Precipitators

The precipitator is a good mixer so the slurry temperature, density and specific heat capacity at constant pressure in the precipitator are the same as that of the outflow. The outlet temperature of the precipitator equals the inlet temperature of the downstream precipitator. The dynamic heat balance in the precipitators is shown in the following equation:

$$c_p V \rho \frac{dT_i}{dt} = c_p F \rho T_{i-1} - c_p F \rho T_i - c_{p,w} \rho_w F_{wi} (T_{wi,out} - T_{wi,in}) - Q_i - \Delta H_i \quad (1)$$

where i is the precipitator number; V the slurry volume in the precipitator; c_p the slurry specific heat at constant pressure; ρ the slurry density; F the slurry flow rate through the precipitator; T_i the outlet temperature of the ith precipitator; T_0 the feed temperature of the first precipitator; $c_{p,w}$ the specific heat of the cooling water; ρ_w the density of the cooling water; F_{wi} the cooling water flow rate through the ith heat exchanger; $T_{wi,in}$ the cooling water inlet temperature of the ith heat exchanger; $T_{wi,out}$ the cooling water outlet temperature of the ith heat exchanger; Q_i the heat dissipation capacity per unit time; ΔH_i the enthalpy of crystallization reaction per unit time.

Eqs.(1) is nonlinear, because it contains the product of variables F_{wi} and $(T_{wi,out} - T_{wi,in})$. Attaining a heat equilibrium in a heat exchanger is much sooner than that in a precipitator. Therefore the heat transfer process in the heat exchanger can be expressed by a static model.

3.2 Static Model of The Heat Exchanger

The time constant of the heat balance in a precipitator is about several hours, but the time constant of the heat transfer in a plate heat exchanger is only a few seconds. Therefore, the heat exchanger dynamics can be grasped with a static model. The total rate of heat transfer between the hot and cold fluids passing through a plate heat exchanger may be expressed as:

$$Q_w = c_{p,w} \rho_w F_w (T_{w,out} - T_{w,in}) = c_p \rho F_a (T_{a,in} - T_{a,out}) = UA\Delta t_m \quad (2)$$

where Q_w the heat transferred in the heat exchanger; F_a is the slurry flow rate through the heat exchanger; $T_{a,in}$ the slurry inlet temperature of the heat exchanger; $T_{a,out}$ the slurry outlet temperature of the heat exchanger; U the total heat transfer coefficient of the heat exchanger; A the total heat exchange area of the heat exchanger; Δt_m the log mean temperature difference. The wide-runner plate heat exchanger is a kind of counter-flow heat exchanger, which means the two fluids enter the heat exchanger from the opposite ends. The log mean temperature difference is defined by the logarithmic mean as following:

$$\Delta t_m = \frac{(T_{a,out} - T_{w,in}) - (T_{a,in} - T_{w,out})}{\ln(\frac{T_{a,out} - T_{w,in}}{T_{a,in} - T_{w,out}})} \quad (3)$$

From Equations (2) and (3):

$$T_{w.out}=\frac{(\exp(\frac{UA}{F_w c_{p,w}}-\frac{UA}{F_a c_p})-1)T_{ai,in}+\frac{F_w c_{p,w}}{UA}T_{w,in}}{\frac{F_w c_{p,w}}{UA}+\exp(\frac{UA}{F_w c_{p,w}}-\frac{UA}{F_a c_p})-1} \quad (4)$$

The overall heat transfer coefficient U takes into account the individual heat transfer coefficients of each fluid and the resistance of the wall material. In order to ensure the high efficiency of the heat exchange and simplify the control operation, the slurry flow rate through the exchanger is kept at an almost constant level in actual operation. Hence the slurry heat transfer coefficient is an almost constant. This means the total heat transfer coefficient only changes with the cooling water flow rate. It can be calculated as (Liu,2013a):

$$U=1/(\theta_1+\theta_2/F_w^{\theta_3}) \quad (5)$$

Where θ_1, θ_2, θ_3 are unknown parameters, and are all almost constants under normal production conditions. These parameters are difficult to be determined directly, they need to be identified using the practical process data.

3.3 Hammerstein Model of Precipitation Process

The Hammerstein model consists of a static input nonlinearity block in series with a dynamic linear block. Let $v_i=(T_{wi,out}-T_{wi,in})F_{wi}$. The whole precipitation process can be described by a series of Hammerstein models as:

$$\frac{dT_i}{dt}=\frac{F}{V}T_{i-1}-\frac{F}{V}T_i-\frac{\rho_w c_{p,w}}{\rho V c_p}v_i-\frac{\Delta H_i+Q_i}{\rho V c_p} \quad (6)$$

$$v_i=f(F_{wi},T_{ai,in},T_{wi,in},F_{ai})=\frac{(\exp(\frac{U_i A}{F_{wi}c_{p,w}}-\frac{U_i A}{F_{ai}c_p})-1)(T_{ai,in}-T_{wi,in})F_{wi}}{\frac{F_{wi}c_{p,w}}{U_i A}+\exp(\frac{U_i A}{F_{wi}c_{p,w}}-\frac{U_i A}{F_{ai}c_p})-1} \quad (7)$$

4. DECENTRALIZED ADAPTIVE MPC

In order to obtain satisfactory precipitation rates and quality of alumina trihydrate, the decomposition temperature in the last precipitator should be stable at a proper constant and the cooling speed should be steady and the difference between the outlet temperature of the first precipitator and the outlet temperature of the last precipitator should be above 10 degrees. That means the control objective is to adjust the outlet temperature of the different precipitators to be consistent with the setting temperature profile. In the process models (7) and (8), T_i are the desired controlled variables, F_{wi} are the manipulated variables, and ΔH_i, Q_i, F_{ai}, $T_{ai,in}$, $T_{wi,in}$ are the disturbances. Among them ΔH_i and Q_i are difficult to be measured directly or indirectly. Therefore, the control method should be suitable for a large-scale and nonlinear system. Furthermore, this method should be able to account for the major measurable disturbances and the unmeasured disturbances for precision enhancing. In order to decrease the computational complexity and guarantee the performance of overall system at the same time, a decentralized adaptive MPC approach is proposed for decomposition temperature control in the alumina trihydrate precipitation process.

According to the equipment connection pattern, the whole system illustrated in Fig.1 can be divided into five subsystems, and each subsystem includes two precipitators and a heat exchanger except the subsystem only including two precipitators. In fact, due to the absence of the heat exchanger, the outlet temperatures of precipitator 1 and precipitator 2 are uncontrollable. The corresponding model is only used to predict the output temperatures of the subsystem. In other subsystems, the output temperature can be controlled by regulating the cooling water flow of the heat exchangers. Each subsystem MPC controller can be designed individually based on subsystem model. In order to avoid performance loss caused by the decentralized control, the subsystem model accounts the output temperature of the upstream subsystem as a measurable disturbance variable, and the lumped unmeasured disturbances are estimated by an adaptive disturbance model. The closed-loop stability of the whole MPC system could be guaranteed when each local closed-loop system remains stable. The decentralized scheme has no influence on the stability of individual control loops due to the coupling among the subsystems being treated as disturbances, and the realization of a stable control to a simple system is easier than that to a large scale system.

4.1 State Space Model of Subsystems

In industrial application, the measurements are available digitally with a sampling time. Thus the discrete time version of the subsystem is derived by approximating the derivatives using simple Euler approximation. Let state x_i denote T_i, and u_i denote F_{wi}, and d_i denote the measured disturbances F_{ai}, $T_{ai,in}$, $T_{wi,in}$, and w_i denote the unmeasured disturbances. Then the state space representation of subsystem j deduced from the previous equations (6) and (7) can be expressed as:

$$X_j(k+1)=AX_j(k)+BV_j(k)+DX_{j-1}(k)+GW_j(k) \quad (8)$$

Where j is the subsystem number, j=1…5 and i=2j-1;

$X_j(k)=[x_i(k)\quad x_{i+1}(k)]^T$; $x_0(k)=T_0(k)$;

$V_j(k)=[v_i(k)\quad 0]^T$; $v_i(k)=f(u_i(k),d_i(k))$;

$v_1(k)\equiv 0$; $W_j(k)=[w_i(k)\quad w_{i+1}(k)]^T$;

$$A=\begin{bmatrix}-F/V & 0\\ F/V & -F/V\end{bmatrix};\ B=\begin{bmatrix}\rho_w c_{p,w}/(\rho V c_p) & 0\\ 0 & 0\end{bmatrix};$$

$$D=\begin{bmatrix}0 & F/V\\ 0 & 0\end{bmatrix};\ G=\begin{bmatrix}-1/(\rho V c_p) & 0\\ 0 & -1/(\rho V c_p)\end{bmatrix}.$$

4.2 Adaptive Unmeasured Disturbance Model

To achieve offset-free control MPC usually adopts a constant output step disturbance model. The disturbance model is equivalent to assuming an output disturbance that remains

constant for all future time (Lundström). This method is simple and applied widely in industrial model predictive control. In this work we will develop the more sophisticated disturbance model based on the actual system in order to improve the prediction accuracy and hence control performance. In Eq.(8), the unmeasured disturbances $W_j(k)$ can be observed by the follow equation.

$$W_j(k-1) = G^{-1}X_j(k) - G^{-1}(AX_j(k-1) + BV_j(k-1) + DX_{j-1}(k-1)) \quad (9)$$

$W_j(k)$ consist of the measurement noise, the external unmeasured disturbances as well as the effects caused by model mismatches. The enthalpy of crystallization reaction and the heat dissipation capacity are the main external unmeasured disturbances in each precipitator subsystem. Because of the inertia of the heat transfer process, the time series $w_i(k)$ must have some statistical regularity and can be estimated through the regression model described the statistical regularity. After analyzing a large amount of real production data we found that the autocorrelations of the time series $w_i(k)$ show the smear characteristics and that the partial autocorrelations show two order truncated tail characteristics. Therefore, we can describe the disturbances $w_i(k)$ with two order autoregressive model as the following formula:

$$w_i(k) = \varphi_{i0} + \varphi_{i1}w_i(k-1) + \varphi_{i2}w_i(k-2) + \varepsilon(k) \quad (10)$$

Where $\varepsilon(k)$ is a zero mean white noise sequence, and φ_{i0}, φ_{i1}, φ_{i2} are the model parameters. The parameters can be estimated by the historical time series of $w_i(k)$. The model parameters will be re-estimated whenever a new $w_i(k)$ value is obtained, then the new model can be used to predict subsequent disturbances.

4.3 MPC Formulation

Since there are no manipulated variables in subsystem 1, a predictor is applied for estimating the future states. In the predictor, the prediction model is (8), and the measurable disturbance $T_0(k)$ is assumed to be a constant during the estimating of $X_1(k)$.

As for subsystem j=2,3,4,5, the decomposition temperature is controlled by a local MPC. The local MPC is formulated based on Hammerstein predictive model. In this study, we use the two-step control scheme that is easy to calculate and implement (Ding). It first applies the linear MPC to get the desired intermediate variables, and then obtains the actual control action by solving nonlinear algebraic equation. The details of it are presented as follows. The performance index for each subsystem is:

$$J_j(k) = \sum_{t=1}^{P_j} \left\| X_j(k+t|k) - Xr_j(k+t) \right\|_{Q_j}^2 + \sum_{t=1}^{M_j} \left\| \Delta V_j(k+t-1|k) \right\|_{R_j}^2 \quad (11)$$

Where X_{rj} is the setting vector, namely the reference decomposition temperature of subsystem j; ΔV_j is the increment of intermediate variable vector V_j; P_j is the prediction horizon and M_j is the control horizon; Q_j and R_j are the positive definite weighting matrices and have block-diagonal forms. The local optimization problem for subsystem j at the sampling time instant k is:

$$\min_{\Delta v_j(k)} \quad J_j(k), j = 2...5 \quad (12a)$$

$$\text{s.t.} \quad X_j(k|k) = X_j(k) \quad (12b)$$

$$X_j(k+t|k) = AX_j(k+t-1|k) + BV_j(k+t-1|k) + DX_{j-1}(k+t-1|k) + GW_j(k+t-1|k) \quad (12c)$$

$$V_{\min} \le V_j(k) \le V_{\max} \quad (12d)$$

$$\Delta V_{\min} \le \Delta V_j(k) \le \Delta V_{\max} \quad (12e)$$

Where the constraints (12d) and (12e) are determined by real input saturation constraints; $\{V_{\min}, V_{\max}\}$ and $\{\Delta V_{\min}, \Delta V_{\max}\}$ are boundaries of intermediate variables and boundaries of increment of them respectively. In this case sequences $X_j(k)$ and $V_j(k)$ are available, problem (12) can be recast as a quadratic program. At every time step, the optimization problem is solved to get the optimal intermediate variable $V_j^*(k)$, and then the optimal control decision sequence $u_i^*(k)$ is obtained by solving the following nonlinear equation:

$$v_i^*(k) = f(u_i(k), d_i(k)) \quad (13)$$

Solving problem (12) requires the use of the future states of its upstream subsystem and the estimation of unmeasured disturbances. The DMPC algorithm for the overall system is as follows:

1. At time k, measure the state $X_j(k)$, disturbance T_0 and the input $u_i(k\text{-}1)$, and calculate the intermediate variable $V_j(k\text{-}1)$.
2. Observe $W_j(k\text{-}1)$ by the formula (9), and then update the parameters of the model (10), and at last estimate the future disturbance sequences $W_j(t+k\text{-}1)$ (t=1…P_j) by the updated model.
3. Calculate $X_1(t+k\text{-}1)$ (t=1…P_j) by predictor, and solve the problem (12) to derive the optimal intermediate variable $V_j^*(k)$.
4. Solve the nonlinear equation (13) to obtain the control sequences $u_i^*(k)$, and command the first value of the control sequences to the process.
5. Set k=k+1, and return to step 1 at the next sample time.

5. REAL DATA BASED SIMULATIONS

To test the validation of the proposed method, we take an alumina trihydrate precipitation process in an alumina plant located in Jiaozuo Henan China as an example. The operating point data show in Table 1. In all the simulation runs, the process is simulated using the nonlinear first principle model and production data including real disturbances and noise (Liu,2013b).

Table 1. Operating data for precipitation process

Process variable	Description	Operating piont
F ($m^3 \cdot h^{-1}$)	Slurry flow rate	885
V (m^3)	Slurry volume	4308
ρ ($kg \cdot m^{-3}$)	Slurry density	1550
c_p ($J \cdot kg^{-1} \cdot k^{-1}$)	Slurry specific heat	2690
A (m^2)	Heat exchange area	339.6

ρ_w (kg·m^{-3})	Water density	1000
$c_{p,w}$ (J·kg^{-1}·k^{-1})	Water specific heat	4174
F_w (m^3·h^{-1})	Cooling water flow rate	0~400

5.1 Validation of Designed Model

There is little difference between each subsystem model, thus we only take subsystem 2 as an example in this simulation. We identified the undetermined coefficients of the heat exchanger model using historical production data, and then estimated the cooling water outlet temperature by Eqs.(5). In Fig.3 the continuous line shows the real cooling water outlet temperature while the dashed line represents the model out. There exists a little difference in the steady state value, a kind of error which can be easily overcome by a controller with integral action. The dynamics of the estimation matches the real measurement quite well. The outlet temperature of both precipitators are predicted by equation (9), in which the unmeasured item $W_j(k)$ was not computed. Fig.4 and Fig.5 show the decomposition temperature in the precipitator 3 and in precipitator 4 respectively. The curves of predictive results are close to that of measurements, but some obvious differences exist between them. The differences are caused by the unmeasured disturbances. The simulation shows that model (9) is suitable as a local prediction model meanwhile the prediction of unmeasured disturbances is a must.

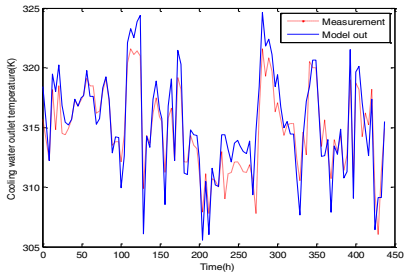

Fig.3 Comparison between the estimative results and the measurement of cooling water outlet temperature ($T_{w3,out}$)

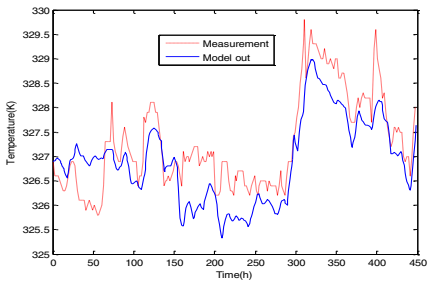

Fig.4 Comparison between the model out and the measurement of T_3

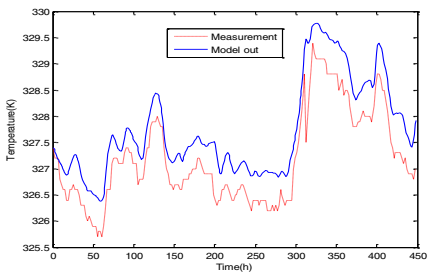

Fig.5 Comparison between the model out and the measurement of T_4

5.2 Performance of Proposed Controllers

As a reference for the performance of the local MPC controller with an adaptive unmeasured disturbance model, a classical MPC controller was also simulated. The classical MPC adopts a constant output step disturbance model to resist unmeasured disturbances. Set the prediction horizon P_j=12, the control horizon M_j=2 and the control sampling period is 1 hour. Fig.6 shows the subsystem closed loop response for step change in the set-point. The performance of the adaptive MPC controller is better than that of the classical MPC controller, as it executes with a smaller overshoot and a stronger rejection of disturbances and a better following of the set-point. Fig.7 demonstrates the performance of the proposed decentralized adaptive MPC regulating all decomposition temperatures. The temperature reference value is set according to the production requirement. In fact, T_1 and T_2 are not controllable, thus there is no need to set the corresponding reference value. The feed temperature (T_0) is determined by the upstream procedure, and it has an approximate step change at time 150h and 300h respectively. The uncontrollable variables T_1 and T_2 follow the fluctuation of T_0 faithfully, and T_2 is higher than T_1 due to the exothermic crystallization. The controlled temperatures (T_3~T_{10}) are maintained at the set-points well. The temperature difference between T_1 and T_{10} is above 10 degrees and the cooling speed is steady. The simulation indicates that the proposed decentralized adaptive MPC method has a good control performance in presence of unmeasured disturbances, and can meet the requirements for the decomposition temperature control.

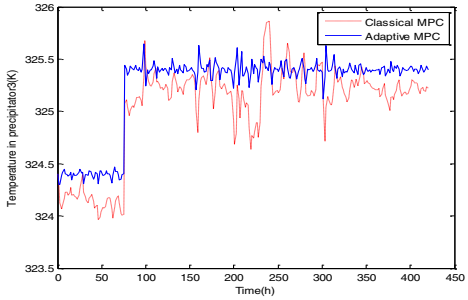

Fig.6 Performances of the adaptive MPC

6. CONCLUSIONS

In this paper, we have proposed a decentralized adaptive MPC approach for controlling the decomposition temperature in precipitation process, in which the large scale nonlinear system is divided into several interconnected subsystems and each subsystem is controlled by a local MPC. To overcome the computational obstacle of nonlinear model, we use the Hammerstein model as the prediction model of each local MPC, and adopt the two-step control algorithm with a small computational burden. Meanwhile an adaptive unmeasured disturbance model is designed to improve the disturbance rejection capability of the local controller. Furthermore, in order to avoid performance loss caused by the decentralized control, the subsystem prediction model accounts the upstream subsystem state as a measurable disturbance. From the simulation studies, it can be concluded that the proposed

approach can ensure a good performance in presence of real disturbances.

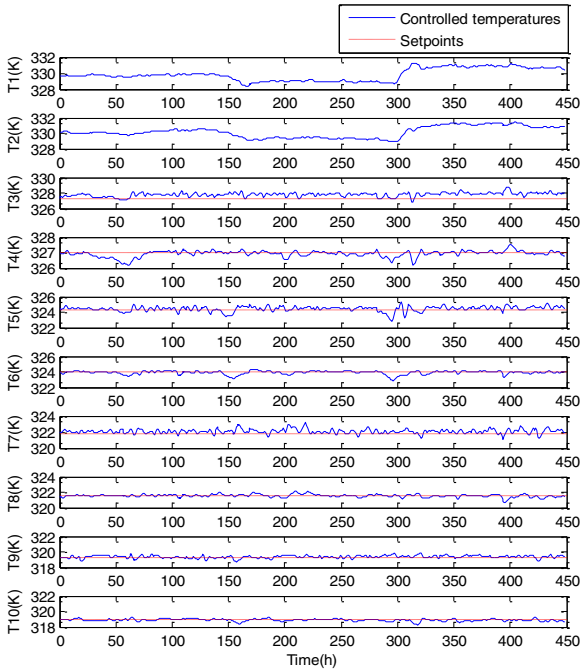

Fig.7 Performance of the decentralized adaptive MPC

ACKNOWLEDGEMENTS

This work was supported by the Nature Science Foundation of China under Grant 61134006, 61273169, 61105080. The real production data using in the simulation were provided by Aluminum Corporation of China Limited.

REFERENCES

Alvarado, I., Limon, D., Muñoz de la Peña, D., Maestre, J. M., Ridao, M. A., Scheu, H., Marquardt, W., Negenborn, R.R., Schutter, B.D., Valencia, F. and Espinosa, J. (2011). A comparative analysis of distributed MPC techniques applied to the HD-MPC four-tank benchmark. *Journal of Process Control,* 21 (5), 800-815.

Christofides, P. D., Scattolini, R., Muñoz de la Peña, D., and Liu, J. (2013). Distributed model predictive control: A tutorial review and future research directions. *Computers and Chemical Engineering,* 51, 21-41.

Ding, B. and Xi, Y. (2006). A two‐step predictive control design for input saturated Hammerstein systems. *International Journal of Robust and Nonlinear Control,* 16 (7), 353-367.

Heidarinejad, M., Liu, J., Muñoz de la Peña, D., Davis, J. F., & Christofides, P. D. (2011a). Handling communication disruptions in distributed model predictive control. *Journal of Process Control,* 21 (1), 173-181.

Heidarinejad, M., Liu, J., Muñoz de la Peña, D., Davis, J. F. and Christofides, P. D. (2011b). Multirate Lyapunov-based distributed model predictive control of nonlinear uncertain systems. *Journal of Process Control,* 21 (9), 1231-1242.

Liu, J., Muñoz de la Peña, D. and Christofides, P. D. (2010). Distributed model predictive control of nonlinear systems subject to asynchronous and delayed measurements. *Automatica,* 46 (1), 52-61.

Liu, Z., Peng, X., Wang, M. and Chen, J. (2013a). Modeling and model predictive control of decomposition temperature in alumina precipitation based on disturbance prediction. The Chinese Journal of Nonferrous Metals, 23 (8), 2309-2315.

Liu, Z. and Peng, X. (2013b). Dynamic modelling for energy transfer process in alumina precipitation. Journal of Central South University, 44 (3), 1037-1042

Lundström, P., Lee, J. H., Morari, M. and Skogestad, S. (1995). Limitations of dynamic matrix control. *Computers and chemical engineering,* 19 (4), 409-421.

Magni, L. and Scattolini, R. (2006). Stabilizing decentralized model predictive control of nonlinear systems. *Automatica,* 42 (7), 1231-1236.

Mercangöz, M. and Doyle III, F. J. (2007). Distributed model predictive control of an experimental four-tank system. *Journal of Process Control,* 17 (3), 297-308.

Mohamed, T. H., Bevrani, H., Hassan, A. A. and Hiyama, T. (2011). Decentralized model predictive based load frequency control in an interconnected power system. *Energy Conversion and Management,* 52 (2), 1208-1214.

Moradzadeh, M., Boel, R. and Vandevelde, L. (2013). Voltage coordination in multi-area power systems via distributed model predictive control. *IEEE Transactions on Power Systems,* 28 (1), 513-521

Qin, S.J. and Badgwell, T.A. (2003). Asurvey of industrial model predictive control technology. *Control Engineering Practice,* 11 (7), 773-764.

Satapathy, B. K. and Vidyasager, P. (1990). Effect of temperature, impurities, retention time and seeding on the rate of crystal growth, nucleation and quality of alumina hydrate during precipitation. *Light Metals*, 1990, 105-113.

Scattolini, R. (2009). Architectures for distributed and hierarchical model predictive control–a review. *Journal of Process Control,* 19(5), 723-731.

Yamada, K. and Yoshihara, M. (1978). Crystallization of aluminum trihydroxide from sodium aluminate solution. *Light Metals,* 1978, 2.

Yanly, X., Qun, Z., Shiwen, B. and Zijian, L. (2002). Effect of precipitating condition and additives on the attrition-resistance property of hydroxide alumina. *Light Metals Warrendale Proceedings*, 149-152.

Wang, C. and Ong, C. J. (2010). Distributed model predictive control of dynamically decoupled systems with coupled cost. *Automatica,* 46 (12), 2053-2058.

XI, Y.G., LI, D.W. and LIN, S. (2013). Model predictive control—status and challenges. *Acta Automatica Sinica,* 39 (3), 224-236.

Zheng, Y., Li, S. and Li, N. (2011). Distributed model predictive control over network information exchange for large-scale systems. *Control engineering practice,* 19 (7), 757-769.

Zheng, Y., Li, S. and Wang, X. (2009). Distributed model predictive control for plant-wide hot-rolled strip laminar cooling process. *Journal of Process Control,* 19 (9), 1427-1437.